

# Position Optimization for Swarm-based UAV-to-UAV Communication Systems

Mingzhi Xu, Kuan Wu<sup>a</sup>, Jianchao Chen<sup>b</sup>, Xiaojing Huang and Ming Jiang<sup>\*c</sup>

*School of Electronics and Information Technology (School of Microelectronics),  
Sun Yat-sen University, Guangzhou, China*

**Keywords:** UAV-to-UAV Communication, UAV Swarm Communication, Relative Position Optimization (RPO), Successive Convex Approximation (SCA), Energy Efficiency (EE).

**Abstract:** Unmanned aerial vehicle (UAV) technologies have played an important role in the beyond-fifth-generation (B5G) networks. To meet the increasing demand for UAV swarm communications, in this paper we propose an intra-swarm UAV-to-UAV (IaS-U2U) communication mechanism for enabling data services in the so-called out-of-coverage (OOC) scenario, where the conventional terrestrial cellular network infrastructure is not available, for example in the cases of mountains, oceans, deserts and forests. Specifically, an optimization problem is formulated by jointly considering the single-pair transmission rate (STR) and the propulsion power (PP), where the UAVs' pairing and relative positioning are taken into account. To solve the complicated joint optimization problem, we decompose it into the UAV pairing process and the relative position optimization (RPO) process, where in the latter a successive convex approximation (SCA) based RPO algorithm is proposed. Simulation results show that the new scheme can provide notable gains in terms of energy efficiency (EE) over selected benchmark methods under different conditions.


## 1 INTRODUCTION


Unmanned aerial vehicle (UAV) technologies have played an important role in the beyond-fifth-generation (B5G) networks. While a single UAV can participate in the cellular network communication as user equipment (UE), a group of autonomous UAVs forming a swarm can provide a higher overall capability and more flexibilities for data services. Thus, UAV swarm technologies have recently attracted increasing attention in the area of UAV communications, targeting the complicated and cooperative tasks such as collaborative surveillance/computing, natural disaster recovery, search and rescue operations and many more applications.


Among the existing issues related to UAV communications, Liu *et al.* (Liu and Lau, 2019) formulated a transmission rate maximization problem considering the interference of users to jointly optimize UAVs' positions, user association, and wireless backhaul capacity allocation. However, the aspect of propulsion energy is also worth considering due to the typically

limited airborne energy at UAVs (Zeng *et al.*, 2019; Ahmed *et al.*, 2020). Zeng *et al.* (Zeng *et al.*, 2019) derived the expression of propulsion power (PP) for rotary-wing UAVs and formulated an energy minimization problem, targeting a joint optimization of UAV trajectory, communication time allocation and task completion latency. Ahmed *et al.* (Ahmed *et al.*, 2020) tried to maximize the throughput under the constraint of energy consumption, involving aspects like UAV trajectory, transmit power and user association. In addition, Ye *et al.* (Ye *et al.*, 2021) investigated an energy-constrained system throughput maximization problem in a scenario, where the UAV charges the internet-of-things (IoT) sensors along its trajectory, based on an energy consumption model for rotary-wing UAVs considering the hovering, flying and charging energy.

However, the aforementioned works only focus on UAV-to-ground (U2G) scenario, which does not involve UAV-to-UAV (U2U) technologies. In U2U scenarios, many technical challenges are foreseen. Ranjha *et al.* (Ranjha and Kaddoum, 2020) discussed the applicability of different access, forward error correction and modulation schemes in multi-hop U2U communication. Du *et al.* (Du *et al.*, 2020) analyzed the

<sup>a</sup>  <https://orcid.org/0000-0003-2448-4604>

<sup>b</sup>  <https://orcid.org/0000-0002-0024-8618>

<sup>c</sup>  <https://orcid.org/0000-0001-9064-7307>

spectrum sensing and sharing problems between the U2U pair and the cellular user. Zhang *et al.* (Zhang *et al.*, 2019) proposed a cooperative UAV sense-and-send protocol for cellular UAVs, and formulated a subchannel allocation and UAV speed optimization problem to maximize the uplink sum-rate. Though, the above schemes do not consider or optimize the UAVs' positions, which however constitute one of the key issues in the context of swarm-based U2U communication systems.

Then, other researchers start to consider U2U solutions involving the UAV's position or trajectory. For example, Wang *et al.* (Wang *et al.*, 2020) attempted to minimize the U2U mission completion time by jointly optimizing the UAVs' trajectories and transmit power using the successive convex approximation (SCA) algorithm. Nevertheless, their approach ignores the quality-of-service (QoS) constraints. Furthermore, note that the techniques of (Zhang *et al.*, 2019) and (Wang *et al.*, 2020) rely on the computing facilities of ground base stations. Thus, they cannot be applied to the so-called out-of-coverage (OOC) scenario defined by the third generation partnership project (3GPP), where terrestrial communication infrastructure is not available. Examples of the OOC scenario can be the cases that when the UAV travels through a humanless area, such as mountains, oceans, deserts and forests.

Noting the representativeness and significance of the OOC scenario for UAV-oriented applications, Chen *et al.* (Chen, 2020) suggested that UAVs may act as relay nodes to assist data communication between terrestrial UEs. They studied a few aspects, for instance the UAVs' positions, transmission power and bandwidth allocation, such that the system transmission rate can be maximized. However, they only focused on the UAVs' individual hovering positions and ignored their interactions as a swarm, thus limiting the potential applications to scenarios without intra-swarm collaborations. Then, realizing the importance of UAV swarming, Hong *et al.* (Hong *et al.*, 2020) proposed a proactive topology-aware routing scheme for the OOC scenario, where the routing is dynamically adjusted based on the swarm's mobility. Nevertheless, they assumed that the relative positions of UAVs change only when the swarm travels close to an obstacle. In other words, the impact on U2U communication from the UAVs' relative positions was ignored (Hong *et al.*, 2020). Moreover, all the aforementioned schemes neglect the PP of UAVs. However, this is among the most critical issues of practical U2U systems, especially in many typical OOC scenarios, where power charging stations are usually unavailable. To address the PP issue in OOC scenar-

ios, it would be beneficial to design an efficient U2U communication mechanism by taking into account the UAVs' energy aspect.

Under the above background, we propose a new scheme for intra-swarm U2U (IaS-U2U) communication in the OOC scenario. The main contributions of our work include:

- Different from many approaches (Zhang *et al.*, 2019; Wang *et al.*, 2020; Chen, 2020) which either assume the support from ground base stations or consider non-swarming UAVs only, we propose a new swarm-based IaS-U2U communication mechanism particularly targeting the OOC scenario.
- To our best knowledge, we appear to be the first to investigate the joint optimization problem of the single-pair transmission rate (STR) and the PP of UAVs under QoS constraints in the OOC scenario. This is different from many existing schemes (Zhang *et al.*, 2019; Hong *et al.*, 2020), where one of or both the STR and PP aspects are not considered. Furthermore, while existing methods such as (Hong *et al.*, 2020) only focus on the UAVs' trajectory, we cast important insights into the impact from the position optimization on the system's attainable performance under a given swarm velocity.
- To solve the joint optimization problem, we first decompose it and then construct an SCA-based relative position optimization (RPO) algorithm, which can provide an initial solution satisfying the complicated QoS constraints, such that the decomposed problem can be iteratively solved.

The rest of the paper is organized as follows. The system model is presented in Section 2. In Section 3, we introduce the proposed IaS-U2U communication mechanism and formulate the joint optimization problem constrained by the QoS requirements. Then in Section 4, the details of the proposed RPO algorithm are provided for solving the target problem. Simulation results and discussions are offered in Section 5, and our conclusions are outlined in Section 6.

## 2 SYSTEM MODEL

In this work, we focus on the transmission issue between the UAVs in the same travelling swarm. Figure 1 shows a UAV swarm deployed in an OOC scenario, where three types of UAVs co-exist. More specifically, the central UAV (C-UAV) is located at the virtual relative center of the swarm with a radius

of  $r_{sw}$ . It is responsible for coordinating and designating a moving trajectory that applies to all UAVs in the swarm, including a total of  $M$  helper UAVs (H-UAV) and  $N$  requester UAVs (R-UAV) besides the C-UAV. We consider a general scenario, where some H-UAVs transmit their stored data packets to specific R-UAVs in the same swarm through selected U2U channel links that satisfy the QoS requirement. In reality, this can be for example the case of collaborative surveillance and computing, where R-UAVs, which have a more powerful computing capability, are responsible for certain analysis or processing based on the input surveillance information collected by H-UAVs with a large cache space and specialized in data sensing.

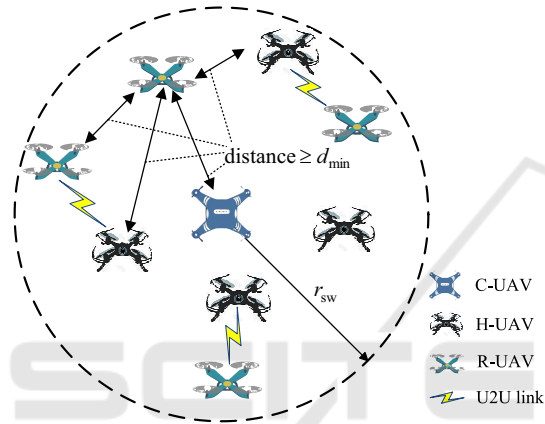


Figure 1: The illustration of the intra-swarm U2U network topology.

Note that the swarm basically is a moving *intranet*, except that all UAVs have satellite navigation functions and thus know their own global positions. Thus, the C-UAV can broadcast its position information at the beginning of each time slot for coordinating the swarm's movement. Other UAVs in the swarm can combine their own global coordinates with the received global coordinates of the C-UAV, so as to deduce their intra-swarm coordinates relative to C-UAV through simple geometric calculations. Furthermore, C-UAV may support satellite communication for exchanging crucial control signalling, such as commands from a remote control center. From the perspective of broadband access, Figure 1 may be viewed as an OOC scenario with no support from conventional terrestrial networks.

As any UAV may take the role of H-UAV or R-UAV in different time depending on specific requirements and conditions, we assume that the H-UAVs and R-UAVs are randomly distributed in the swarm as a generalized example. Furthermore, the distance between any two UAVs is no less than a predefined safety distance  $d_{min}$  to avoid collisions. Moreover,

without loss of generality, we assume that the distance between different swarms is relatively large, such that the inter-swarm interference may be neglected. Though, the intra-swarm interference exists in the swarm under the full frequency reuse factor of one. For simplicity, all UAVs are assumed to fly at the same altitude, thus we may only focus on  $x, y$  directions of the two-dimensional trajectory plane.

Denote  $\mathcal{N} = \{1, \dots, n, \dots, N\}$  and  $\mathcal{M} = \{N+1, \dots, N+m, \dots, N+M\}$  as the sets of the indices of R-UAVs and H-UAVs, respectively. Under the high-altitude airborne environment, the signal propagation between UAVs may be considered following a line-of-sight (LOS) channel (Du et al., 2020; Wang et al., 2020). The channel gain from H-UAV  $m$  to R-UAV  $n$  can be formulated as

$$g_m(\mathbf{w}_n) = \beta \|\mathbf{w}_m - \mathbf{w}_n\|^{-\alpha}, \quad m \in \mathcal{M}, n \in \mathcal{N}, \quad (1)$$

where  $\mathbf{w}_i, \forall i \in \mathcal{M} \cup \mathcal{N}$  is the position of R-UAV  $i$ ,  $\alpha$  is the path loss exponent,  $\beta$  is the channel coefficient and  $\|\cdot\|$  is the  $L_2$ -norm operator. We also assume that the Doppler effect can be reasonably compensated for the swarm.

Compared with fixed-wing UAVs, rotary-wing UAVs are lighter in weight and hence have more flexibilities in practical applications (Zeng et al., 2019; Ahmed et al., 2020; Ye et al., 2021). Thus, in the sequel we formulate the target optimization problem based on the PP model of the rotary-wing UAV, which depends on the UAV's velocity  $V$  (Zeng et al., 2019) as

$$P_p(V) = P_{bla} \left(1 + \frac{3V^2}{U_{tip}^2}\right) + \frac{1}{2} d_{rat} \rho s_{rot} A V^3 + P_{ind} \left(\sqrt{1 + \frac{V^4}{4v_{rot}^4}} - \frac{V^2}{2v_{rot}^2}\right), \quad (2)$$

where  $P_{bla}$  is the blade profile power,  $U_{tip}$  is the tip speed of the rotor blade,  $P_{ind}$  is the induced power,  $v_{rot}$  is the mean rotor induced velocity,  $d_{rat}$  is fuselage drag ratio,  $\rho$  is the air density,  $s_{rot}$  is the rotor solidity, and  $A$  is the rotor disc area (Zeng et al., 2019).

### 3 COMMUNICATION MECHANISM AND PROBLEM FORMULATION

#### 3.1 The Proposed IaS-U2U Communication Mechanism

For better understanding the rationale of our optimization problem to be introduced in Section 3.2, let

us cast more insights into the mechanism of the IaS-U2U system.

Note that in the OOC scenario of Figure 1, the UAVs cannot be managed through the normal way as in terrestrial networks. Thus, compared with the schemes in (Zhang et al., 2019; Wang et al., 2020) where ground base stations are responsible for scheduling U2U transmissions, in our case the C-UAV serves as the centralized node to control the UAV initialization. Then, the proposed RPO algorithm is distributedly executed by each of the R-UAVs in a sequential order, such that their positions can be optimized. In Figure 2, the IaS-U2U communication mechanism tailored for the OOC scenario is portrayed, which is outlined as follows:

1. First, each R-UAV broadcasts the U2U request (3GPP, 2020) and the content feature information (CFI) associated with its targeted data to all H-UAVs. Then, each H-UAV broadcasts the CFI of its cached data. Each R-UAV performs distributed pairing trials with each H-UAV.
2. Every successfully paired R-UAV sends its pairing result to C-UAV, which then combines all received results to form a pairing list. Subsequently, C-UAV initiates the RPO procedure at R-UAVs through a polling strategy as follows:
  - (a) C-UAV sends a position information list containing the coordinates of all H-UAVs and R-UAVs, and the pairing list to the polled R-UAV  $n$ , which then executes the RPO algorithm.
  - (b) R-UAV  $n$  reports the optimization result information, which contains the pairing status (success or failure) and the RPO solution, to C-UAV and its paired H-UAV.
    - i. If the optimization fails, both H-UAV and R-UAV will wait for the next round of pairing.
    - ii. Otherwise, R-UAV  $n$  moves to the new position, and then reports a movement completion message to its paired H-UAV and C-UAV.
  - (c) C-UAV initiates the RPO procedure at the next available R-UAV in a random order, if there remains any.
3. Finally, after all paired R-UAVs are polled, each moved R-UAV establishes U2U connection with its paired H-UAV.

Based on the mechanism of Figure 2 designed for the OOC scenario, our main objective is then to determine the UAV pairing, and to find out to which optimized positions R-UAVs should move, such that qualified U2U connections can be established for the targeted H-UAV~R-UAV pairs.

### 3.2 Problem Formulation

In this subsection, we first present the PP and STR models, and then formulate the corresponding joint optimization problem for the IaS-U2U communication system concerned. Define a binary matrix  $\mathbf{X} = [x_{m,n}]_{(N+M) \times N}$ , where  $x_{m,n} = 1$  and  $x_{m,n} = 0$  denote that H-UAV  $m$  pairs and does not pair with R-UAV  $n$ , respectively. We assume that each H-UAV can serve at most one R-UAV and each R-UAV can only be served by at most one H-UAV, namely

$$\begin{cases} \text{C1: } \sum_{n \in \mathcal{N}} x_{m,n} \leq 1, \forall m \in \mathcal{M} \\ \text{C2: } \sum_{m \in \mathcal{M}} x_{m,n} \leq 1, \forall n \in \mathcal{N} \end{cases} \quad (3)$$

Different from (Hong et al., 2020) which only focuses on the UAV's pairing without considering the impact from their positions, in this work we try to explore the opportunity of exploiting the intra-swarm movements of UAVs for potential performance enhancements. For R-UAV  $n$ , we denote  $\mathbf{w}_n^{\text{start}}$  and  $\mathbf{w}_n$  as its initial position before time slot  $\delta$  and the final position after time slot  $\delta$ , respectively. Since we focus on the RPO process at R-UAVs, we assume that H-UAVs and C-UAV fly at the same velocity, which is defined as the swarm velocity  $\mathbf{v}^{\text{sw}} = [v_x^{\text{sw}}, v_y^{\text{sw}}]^T$ , where  $v_x^{\text{sw}}$  and  $v_y^{\text{sw}}$  denote the swarm velocity in  $x$  and  $y$  directions, respectively. Thus, we may define the velocity vector of R-UAV  $n$  as

$$\mathbf{v}_n = \frac{\mathbf{w}_n - \mathbf{w}_n^{\text{start}}}{\delta} + \mathbf{v}^{\text{sw}}. \quad (4)$$

Then, despite that many existing works (Wang et al., 2020; Chen, 2020; Hong et al., 2020) ignore the PP of UAVs in their designs, it is desirable to consider its potential impact on the performance of the IaS-U2U system, where the energy aspect is a critical constraint, especially in many OOC scenarios typically without power charging facilities. According to (2), the PP of R-UAV  $n$  can be expressed as

$$\begin{aligned} P_p(\mathbf{w}_n) = & P_{\text{bla}} \left( 1 + \frac{3\|\mathbf{v}_n\|^2}{U_{\text{tip}}^2} \right) \\ & + \frac{1}{2} d_{\text{rat}} \rho s_{\text{rot}} A \|\mathbf{v}_n\|^3 + P_{\text{ind}} I_1(\mathbf{v}_n), \end{aligned} \quad (5)$$

where

$$I_1(\mathbf{v}_n) = \left( \sqrt{1 + \frac{\|\mathbf{v}_n\|^4}{4v_{\text{rot}}^4}} - \frac{\|\mathbf{v}_n\|^2}{2v_{\text{rot}}^2} \right)^{\frac{1}{2}}. \quad (6)$$

Furthermore, assuming a frequency reuse factor of unity, we define the STR from H-UAV  $m$  to R-UAV  $n$  in the IaS-U2U communication as

$$R(\mathbf{w}_n) = B \log_2 \left[ 1 + \frac{P_m g_m(\mathbf{w}_n)}{B\epsilon + \sum_{j \in \mathcal{M} \setminus m} P_j g_j(\mathbf{w}_n)} \right], \quad (7)$$

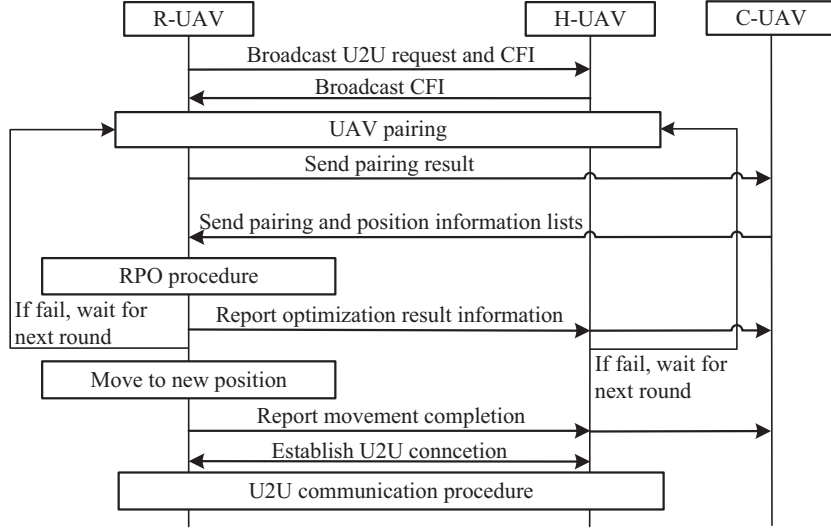


Figure 2: The proposed IaS-U2U communication mechanism.

where we take into account the U2U interference,  $\sum_{j \in \mathcal{M} \setminus m} P_j g_j(\mathbf{w}_n)$ , which is often ignored in the existing literature (Wang et al., 2020; Chen, 2020; Hong et al., 2020), while  $B$ ,  $\varepsilon$  and  $p_m$  denote the system bandwidth, the noise power spectrum density and the transmit power of H-UAV  $m$ , respectively. In addition, we define the total PP of R-UAVs,  $P_p^{\text{tot}}$ , the total STR of H-UAVs,  $R^{\text{tot}}$ , and the system energy efficiency (EE),  $\mu$ , as

$$P_p^{\text{tot}} = \sum_{n \in \mathcal{N}} P_p(\mathbf{w}_n), \quad (8a)$$

$$R^{\text{tot}} = \sum_{m \in \mathcal{M}} \sum_{n \in \mathcal{N}} x_{m,n} R(\mathbf{w}_n), \quad (8b)$$

$$\mu = \frac{R^{\text{tot}}}{P_p^{\text{tot}}}. \quad (8c)$$

respectively, where  $\mu$  is a metric used for performance evaluation purpose.

Therefore, to reflect the aspects of both the PP and the STR, we combine (5) and (7) to form a joint objective function for the IaS-U2U communication system, formulated as

$$U(\mathbf{X}, \mathbf{W}_{\text{R-UAV}}) = \sum_{m \in \mathcal{M}} \sum_{n \in \mathcal{N}} x_{m,n} [R(\mathbf{w}_n) - \theta_n \varphi P_p(\mathbf{w}_n)]. \quad (9)$$

Then, our target optimization problem can be represented by

$$\text{P1: } \max_{\{\mathbf{X}, \mathbf{W}_{\text{R-UAV}}\}} U(\mathbf{X}, \mathbf{W}_{\text{R-UAV}}) \quad (10)$$

subjected to (3) and

$$\begin{cases} \text{C3: } \|\mathbf{v}_n\| \leq V_{\max}, \forall n \in \mathcal{N} \\ \text{C4: } \|\mathbf{w}_n\| \leq r_{\text{sw}}, \forall n \in \mathcal{N} \\ \text{C5: } R(\mathbf{w}_n) \geq R_{\min} \text{ for } x_{m,n} = 1, \forall m \in \mathcal{M}, \forall n \in \mathcal{N}, \\ \text{C6: } \|\mathbf{w}_i - \mathbf{w}_j\| \geq d_{\min}, \forall i, j \in \mathcal{M} \cup \mathcal{N}, i \neq j \\ \text{C7: } \|\mathbf{w}_n\| \geq d_{\min}, \forall n \in \mathcal{N} \end{cases} \quad (11)$$

where  $\mathbf{W}_{\text{R-UAV}} = [\mathbf{w}_1, \dots, \mathbf{w}_N]$  denotes the position matrix of R-UAVs,  $\theta_n \in (0, 1]$  represents the priority factor of R-UAV  $n$ , which is used to adjust the impact of the PP term in the joint optimization problem, and  $\varphi$  is the calibration factor that ensures the PP to be in the same order of magnitude as well as the same unit as the STR. Moreover, C3 indicates the maximum R-UAV velocity  $V_{\max}$ , C4 requires that R-UAVs are within the swarm area, C5 applies the QoS constraint of the minimum STR  $R_{\min}$  for the radio link between the paired H-UAV and R-UAV, and C6/C7 are anti-collision constraints.

Note that P1 in (10) is a typical mixed-integer non-linear programming (MINLP) problem, which is non-convex because  $\mathbf{X}$  is a discrete variable. To solve P1, we propose to first decompose it into the UAV pairing process and the RPO process, and then to solve it in a distributed way.

## 4 THE PROPOSED SOLUTION

### 4.1 The UAV Pairing Process

Based on Figure 2, a UAV obtains other UAVs' CFI before invoking the UAV pairing process. To ensure

that C3 in (11) is satisfied after UAV pairing, it is necessary to down-select the candidate H-UAVs, which can be achieved as follows.

Intuitively, the higher similarity between the data requested by R-UAV  $n$  and the data cached at H-UAV  $m$ , the higher possibility of establishing a U2U connection between R-UAV  $n$  and H-UAV  $m$  should be. Thus, each UAV first calculates the packet content similarities associated with its candidate UAVs based on the Jaccard coefficient, which is a popular metric designed for measuring the similarity between two entities (Niwattanakul et al., 2013), to generate a pairing preference list. Then, R-UAV  $n$  measures the signal-to-interference-plus-noise ratio (SINR) for each H-UAV and removes those below the average SINR from its pairing preference list. Subsequently, during the pairing procedure described in Section 3.1, the classic distributed pairing approach, namely the Gale-Shapley (GS) algorithm (Gusfield and Irving, 1989), can be applied to achieve one-to-one pairing between R-UAVs and H-UAVs, yielding the pairing matrix solution  $\mathbf{X}^*$ . After setting the transmit power of unpaired H-UAVs to zero, each paired R-UAV can invoke the RPO process below in a sequential order and solves P1 in a distributed way.

## 4.2 The Proposed RPO Process

After the pairing matrix is determined, the successfully paired R-UAV  $n$  needs to solve the following problem in the RPO process

$$P2: \max_{\mathbf{w}_n} U_n(\mathbf{w}_n) = \max_{\mathbf{w}_n} [R(\mathbf{w}_n) - \theta_n \phi P_p(\mathbf{w}_n)], \quad (12)$$

subjected to

$$\begin{cases} \text{C8: } \|\mathbf{v}_n\| \leq V_{\max} \\ \text{C9: } \|\mathbf{w}_n\| \leq r_{\text{sw}} \\ \text{C10: } R(\mathbf{w}_n) \geq R_{\min} \\ \text{C11: } \|\mathbf{w}_n - \mathbf{w}_j\| \geq d_{\min}, \forall j \in \mathcal{M} \cup \mathcal{N} \setminus n \\ \text{C12: } \|\mathbf{w}_n\| \geq d_{\min} \end{cases}, \quad (13)$$

where  $U_n(\mathbf{w}_n)$  denotes the objective function of R-UAV  $n$ , and C8-C12 are the constraints similar to those in (11), but applying to this specific R-UAV  $n$ . Note that P2 is non-concave and C10-C12 are non-convex. To solve P2, the objective function and its constraints may have to be slackened. Similar to (Zeng et al., 2019), we introduce a slack variable  $\tau$

$$\text{C13: } \tau \geq I_1(\mathbf{v}_n), \quad (14)$$

where  $I_1(\mathbf{v}_n)$  is defined in (6). Then, by replacing  $I_1(\mathbf{v}_n)$  with its upper bound  $\tau$  given in (14),  $P_p(\mathbf{w}_n)$

in (5) can be approximated by the convex function

$$\begin{aligned} \tilde{P}_p(\mathbf{w}_n, \tau) = & P_{\text{bla}} \left( 1 + \frac{3\|\mathbf{v}_n\|^2}{U_{\text{tip}}^2} \right) \\ & + \frac{1}{2} d_{\text{rat}} \rho_{\text{Srot}} A \|\mathbf{v}_n\|^3 + P_{\text{ind}} \tau. \end{aligned} \quad (15)$$

Hence, based on (15), P2 can be reformulated to

$$P3: \max_{\{\mathbf{w}_n, \tau\}} [R(\mathbf{w}_n) - \theta_n \phi \tilde{P}_p(\mathbf{w}_n, \tau)], \text{ s.t. C8-C13}, \quad (16)$$

where the term  $-\theta_n \phi \tilde{P}_p(\mathbf{w}_n, \tau)$  is concave (Zeng et al., 2019). Then, we have:

**Proposition 1.** *P3 is equivalent to P2.*

**Proof 1.** When  $\tau > I_1(\mathbf{v}_n)$ , to maximize P3, we may decrease the value of  $\tau$  in (14), such that the value of  $\tilde{P}_p(\mathbf{w}_n, \tau)$  in (16) can be reduced, until the equal sign of (14) holds to yield  $P_p(\mathbf{w}_n) = \tilde{P}_p(\mathbf{w}_n, \tau)$ . Then, P3 is equivalent to P2. The proof completes.

To tackle the non-convex C13, we may first square (14) to get  $\tau^2 \geq I_1^2(\mathbf{v}_n)$ , which is then summed up with its reciprocal to yield  $\tau^2 + \frac{\|\mathbf{v}_n\|^2}{v_{\text{rot}}^2} \geq \frac{1}{\tau^2}$  by exploiting  $I_1(\mathbf{v}_n)$  defined in (6). Next, we perform the first-order Taylor expansion on  $\tau^2$  and  $\frac{\|\mathbf{v}_n\|^2}{v_{\text{rot}}^2}$  at  $\tau = \tau^{(k)}$  and  $\mathbf{v}_n = \mathbf{v}_n^{(k)}$ , respectively, such that C13 can be slackened to the following convex constraint

$$\text{C14: } T_1(\tau; \tau^{(k)}) + T_2(\mathbf{v}_n; \mathbf{v}_n^{(k)}) \geq \frac{1}{\tau^2}, \quad (17)$$

where

$$\begin{aligned} T_1(\tau; \tau^{(k)}) &= (\tau^{(k)})^2 + 2\tau^{(k)}(\tau - \tau^{(k)}) \\ T_2(\mathbf{v}_n; \mathbf{v}_n^{(k)}) &= -\frac{\|\mathbf{v}_n^{(k)}\|^2}{v_{\text{rot}}^2} + \frac{2}{v_{\text{rot}}^2}(\mathbf{v}_n^{(k)}) \bullet \mathbf{v}_n \end{aligned} \quad (18)$$

with  $\bullet$  being the vector inner product operator, and  $(\cdot)^{(k)}$  denotes the variable obtained at the  $k$ -th ( $k = 0, \dots, K_{\max}$ ) iteration with  $k = 0$  being the index of the initial solution and  $K_{\max}$  being the maximum number of iterations. According to the definition of  $\mathbf{v}_n$  and the slack variable value formula in (Zeng et al., 2019), for a given  $\mathbf{w}_n^{(k)}$ , we may calculate  $\tau^{(k)}$  by

$$\tau^{(k)} = I_1(\mathbf{v}_n^{(k)}), \quad (19)$$

where

$$\mathbf{v}_n^{(k)} = \frac{\mathbf{w}_n^{(k)} - \mathbf{w}_n^{\text{start}}}{\delta} + \mathbf{v}^{\text{sw}}. \quad (20)$$

Furthermore, since  $\|\mathbf{a}\| \|\mathbf{b}\| \geq \mathbf{a} \bullet \mathbf{b}$ , C11 and C12 can be slackened to the convex constraints C15 and C16, respectively

$$\begin{cases} \text{C15: } (\mathbf{w}_n^{(k)} - \mathbf{w}_j) \bullet (\mathbf{w}_n - \mathbf{w}_j) \\ \quad \geq d_{\min} \|\mathbf{w}_n^{(k)} - \mathbf{w}_j\|, \forall j \in \mathcal{M} \cup \mathcal{N} \setminus n. \\ \text{C16: } \mathbf{w}_n^{(k)} \bullet \mathbf{w}_n \geq d_{\min} \|\mathbf{w}_n^{(k)}\| \end{cases} \quad (21)$$

In addition, note that P3 and C10 are non-convex because the function  $R(\mathbf{w}_n)$  defined in (7) is non-concave. Similar to the first-order Taylor expansion on  $\log(a+y)$  at  $y=y^{(k)}$ ,  $R(\mathbf{w}_n)$  may be approximated by  $\hat{R}(\mathbf{w}_n; \mathbf{w}_n^{(k)})$ , due to

$$\hat{R}(\mathbf{w}_n; \mathbf{w}_n^{(k)}) = R(\mathbf{w}_n^{(k)}) + I_2^{(k)} \left[ \sum_{l \in \mathcal{M}} p_l g_l(\mathbf{w}_n) - g^{(k)} \right] - I_3^{(k)} \left[ \sum_{j \in \mathcal{M} \setminus m} p_j g_j(\mathbf{w}_n) - g_{-m}^{(k)} \right], \quad (22)$$

$$\text{where } I_2^{(k)} = \frac{B \log_2 e}{B\epsilon + g^{(k)}}, \quad I_3^{(k)} = \frac{B \log_2 e}{B\epsilon + g_{-m}^{(k)}}, \quad g^{(k)} =$$

$\sum_{l \in \mathcal{M}} p_l g_l(\mathbf{w}_n^{(k)})$  and  $g_{-m}^{(k)} = \sum_{j \in \mathcal{M} \setminus m} p_j g_j(\mathbf{w}_n^{(k)})$ . To deal with the non-concavity of  $g_l(\mathbf{w}_n)$  and  $g_j(\mathbf{w}_n)$  in (22), we follow (Liu and Lau, 2019) to perform the first-order Taylor expansion on  $g_l(\mathbf{w}_n)$  and  $g_j(\mathbf{w}_n)$  at  $\|\mathbf{w}_n - \mathbf{w}_l\|^\alpha = \|\mathbf{w}_n^{(k)} - \mathbf{w}_l\|^\alpha$  and  $\mathbf{w}_n = \mathbf{w}_n^{(k)}$ , respectively, yielding

$$\left\{ \begin{array}{l} g_l(\mathbf{w}_n) \approx \tilde{g}_l'(\mathbf{w}_n; \mathbf{w}_n^{(k)}) \\ \quad = \frac{2\|\mathbf{w}_n^{(k)} - \mathbf{w}_l\|^\alpha - \|\mathbf{w}_n - \mathbf{w}_l\|^\alpha}{\beta^{-1}\|\mathbf{w}_n^{(k)} - \mathbf{w}_l\|^\alpha} \\ g_j(\mathbf{w}_n) \approx \tilde{g}_j''(\mathbf{w}_n; \mathbf{w}_n^{(k)}) \\ \quad = \frac{\|\mathbf{w}_n^{(k)} - \mathbf{w}_j\|^2 - \alpha(\mathbf{w}_n^{(k)} - \mathbf{w}_j) \bullet (\mathbf{w}_n - \mathbf{w}_n^{(k)})}{\beta^{-1}\|\mathbf{w}_n^{(k)} - \mathbf{w}_j\|^{\alpha+2}} \end{array} \right., \quad (23)$$

where  $\tilde{g}_l'(\mathbf{w}_n; \mathbf{w}_n^{(k)})$  is a concave function and  $\tilde{g}_j''(\mathbf{w}_n; \mathbf{w}_n^{(k)})$  is an affine function. According to (23),  $\hat{R}(\mathbf{w}_n)$  may be further approximated by the following convex function (Chi et al., 2017)

$$\begin{aligned} \tilde{R}(\mathbf{w}_n; \mathbf{w}_n^{(k)}) &\approx R(\mathbf{w}_n^{(k)}) \\ &+ I_2^{(k)} \left[ \sum_{l \in \mathcal{M}} p_l \tilde{g}_l'(\mathbf{w}_n; \mathbf{w}_n^{(k)}) - g^{(k)} \right] \\ &- I_3^{(k)} \left[ \sum_{j \in \mathcal{M} \setminus m} p_j \tilde{g}_j''(\mathbf{w}_n; \mathbf{w}_n^{(k)}) - g_{-m}^{(k)} \right]. \end{aligned} \quad (24)$$

Therefore, C10 may be slackened to the convex constraint

$$\text{C17: } \tilde{R}(\mathbf{w}_n; \mathbf{w}_n^{(k)}) \geq R_{\min}. \quad (25)$$

Thus, we may replace  $R(\mathbf{w}_n)$  in (16) by its approximated version  $\tilde{R}(\mathbf{w}_n; \mathbf{w}_n^{(k)})$  in (24), as well as replace constraints C10 and C11/C12 in (13) by their slackened versions, C17 in (25) and C15/C16 in (21), respectively. Then, P3 may be further reformulated to a new convex problem

$$\begin{aligned} \text{P4: } &\max_{\{\mathbf{w}_n, \tau\}} \tilde{U}_n(\mathbf{w}_n, \tau; \mathbf{w}_n^{(k)}) \\ &= \max_{\{\mathbf{w}_n, \tau\}} [\tilde{R}(\mathbf{w}_n; \mathbf{w}_n^{(k)}) - \theta_n \varphi \tilde{P}_p(\mathbf{w}_n, \tau)], \end{aligned} \quad (26)$$

subjected to C8, C9 and C14-C17.

Next, we can apply the SCA algorithm (Chi et al., 2017) to solve P3 by iteratively solving P4 until convergence. In the first iteration of solving P4, we need to provide an initial solution satisfying the constraints of the original problem, namely P2. However, due to C10, it is difficult to prove P2 is feasible and to find the initial solution directly. Hence, we temporarily ignore C10 and the PP term in P2 to construct a transitional STR maximization (STRM) problem as

$$\text{P5: } \max_{\{\mathbf{w}_n\}} R(\mathbf{w}_n), \text{ s.t. C8, C9, C11, C12.} \quad (27)$$

Note that P5 is a simplified version of P2 and hence the aforementioned operations in (21) and (24) are also applicable. Then, P5 can be transformed to a convex problem

$$\text{P6: } \max_{\{\mathbf{w}_n\}} \tilde{R}(\mathbf{w}_n; \mathbf{w}_n^{(k)}), \text{ s.t. C8, C9, C15, C16.} \quad (28)$$

Then, we use  $\mathbf{w}_n^{(0)} = \mathbf{w}_n^{\text{start}}$  as the initial solution to solve P6 iteratively by the SCA algorithm, such that the maximum STR,  $R_{\max}^{m,n}$ , and a local optimal solution of P5,  $\mathbf{w}_n^{\text{tmp}}$ , can be obtained later. Thus, we have two cases:

- If  $R_{\max}^{m,n} \geq R_{\min}$ , P2 is feasible, implying that  $\mathbf{w}_n^{\text{tmp}}$  satisfies the QoS-related C10 of (13) and the equivalent problem P3 also has a feasible solution according to Proposition 1. Then,  $\mathbf{w}_n^{\text{tmp}}$  can be used to construct the initial solution of P4 as  $\{\mathbf{w}_n^{(0)}, \tau^{(0)}\}$ , where  $\mathbf{w}_n^{(0)} = \mathbf{w}_n^{\text{tmp}}$  and  $\tau^{(0)}$  is calculated by (19). P4 is then solved iteratively to achieve a local optimal solution  $\mathbf{w}_n^*$  of P2.
- If  $R_{\max}^{m,n} < R_{\min}$ , P2 is infeasible, indicating that the RPO operation of R-UAV  $n$  fails. Then, R-UAV  $n$  should stay at its initial position  $\mathbf{w}_n^{\text{start}}$  relative to C-UAV and wait for the next round of RPO.

We summarize the above operations in Algorithm 1, where  $\Delta$  denotes a predefined accuracy indicator.

## 5 SIMULATION AND COMPLEXITY ANALYSIS

### 5.1 Simulation Results

In this subsection, the performance results of the proposed RPO scheme are provided, which were generated through MATLAB-based simulations and averaged over a number of trails. Note that for the IaS-U2U communication under the OOC scenario studied

Algorithm 1: The Proposed RPO Algorithm.

---

```

1: Input:  $\mathbf{w}_n^{\text{start}}, K_{\max}, R_{\min}, \Delta$ 
2: //Stage 1: STRM optimization
3:  $\mathbf{w}_n^{(0)} = \mathbf{w}_n^{\text{start}}, k = 0$ 
4: repeat
5:   Solve P6 to obtain the optimal solution  $\mathbf{w}_n^{\text{tmp}}$ 
6:    $\mathbf{w}_n^{(k+1)} = \mathbf{w}_n^{\text{tmp}}$ 
7:    $k = k + 1$ 
8: until  $\left| \frac{R(\mathbf{w}_n^{(k)}) - R(\mathbf{w}_n^{(k-1)})}{R(\mathbf{w}_n^{(k)})} \right| < \Delta$  or  $k = K_{\max}$ 
9: Set  $R_{\max}^{m,n} = R(\mathbf{w}_n^{\text{tmp}})$ , where  $\mathbf{w}_n^{\text{tmp}}$  is a solution to P5
10: if  $R_{\max}^{m,n} \geq R_{\min}$  then
11:   //Stage 2: Joint optimization
12:    $\mathbf{w}_n^{(0)} = \mathbf{w}_n^{\text{tmp}}$ 
13:   Calculate  $\tau^{(0)}$  by (19)
14:    $k = 0$ 
15:   repeat
16:     Solve P4 to obtain its optimal solution  $\mathbf{w}_n^*$ 
17:      $\mathbf{w}_n^{(k+1)} = \mathbf{w}_n^*$ 
18:     Calculate  $\tau^{(k+1)}$  by (19)
19:      $k = k + 1$ 
20:   until  $\left| \frac{U_n(\mathbf{w}_n^{(k)}) - U_n(\mathbf{w}_n^{(k-1)})}{U_n(\mathbf{w}_n^{(k)})} \right| < \Delta$  or  $k = K_{\max}$ 
21: else
22:   Current RPO operation at R-UAV  $n$  fails  $\Rightarrow$ 
   set  $\mathbf{w}_n^* = \mathbf{w}_n^{\text{start}}$ 
23: end if
24: Output:  $\mathbf{w}_n^*$ 

```

---

in this work, there exist few directly comparable reference schemes. Hence, we use the following adapted benchmarks:

1. *The PP minimization (PPM) scheme:* It is obtained by adapting the STR model and constraints of (Zeng et al., 2019) to fit into our scenario. Specifically, we first use the STR model expressed in (7), and then apply the slackening and approximation processes similar to P4 under constraints C8-C12.
2. *The STRM scheme:* It targets solving P5 in (27) only, which does not consider the PP aspect.

Aiming for fair comparison, the UAV pairing process proposed in Section 4.1 and Stage 1 of Algorithm 1 are applied to all schemes. After Stage 1 of Algorithm 1, the PPM scheme minimizes the PP of R-UAVs, while the STRM scheme ignores the U2U pairs not satisfying the QoS-related C10 of (13).

The default values of the main parameters used in our simulations are as follows, unless otherwise stated. The values of PP-related variables are chosen similar to (Zeng et al., 2019) for fair comparison,

namely  $P_{\text{bla}} = 79.865$  W,  $U_{\text{tip}} = 120$  m/s,  $d_{\text{rat}} = 0.6$ ,  $\rho = 1.225$  kg/m<sup>3</sup>,  $s_{\text{rot}} = 0.05$  m<sup>3</sup>,  $A = 0.503$  m<sup>2</sup>,  $P_{\text{ind}} = 88.628$  W and  $v_{\text{rot}} = 4.03$  m/s. The channel parameters are referred to (Wang et al., 2020), namely  $B = 5$  Hz,  $\beta = -60$  dB,  $\alpha = 2$  and  $\epsilon = -170$  dBm/Hz. Others parameters are  $\mathbf{v}^{\text{sw}} = [0, 20]^T$  m/s,  $V_{\text{max}} = 45$  m/s (3GPP, 2017),  $p_m = 0.2$  W,  $\forall m \in \mathcal{M}$  (3GPP, 2017),  $K_{\max} = 10$ ,  $\Delta = 0.1$ ,  $\varphi = 0.15$  Mbit/s/W,  $R_{\min} = 4$  Mbit/s (3GPP, 2019),  $M = 5$ ,  $N = 5$ ,  $\delta = 0.5$  s,  $r_{\text{sw}} = 25$  m,  $d_{\min} = 2$  m and  $\theta_n = 0.5$ ,  $\forall n \in \mathcal{N}$  (Zhu et al., 2019).

Note that the UAV swarms' velocity has a large impact on various aspects of the IaS-U2U communication, as seen in Figure 3. For example, when the swarm velocity  $\|\mathbf{v}^{\text{sw}}\|$  increases, Figure 3a indicates that the total PP of R-UAVs  $P_p^{\text{tot}}$  first increases and then reduces. The phenomenon is consistent with the trend of PP with different velocities observed in (Zeng et al., 2019). More specifically:

- On the one hand, Figure 3a shows that when the swarm is at a low velocity,  $P_p^{\text{tot}}$  reduces as the safety distance  $d_{\min}$  increases. According to (7), a higher  $d_{\min}$  may extend the distance between R-UAVs and H-UAVs and hence decrease the STR. This thus results in a growing proportional impact from PP to the joint objective function given by (9). Thus, the algorithm tends to mitigate the PP for leveraging the maximization of (9) as required by (10).
- On the other hand, however, according to C3 and C7 in (11), a higher swarm velocity with a larger  $d_{\min}$  may make it more challenging for R-UAVs to fulfil the QoS-related constraints, and hence may reduce the number of qualified U2U pairs. Then, while the algorithm tends to reduce PP to exchange for a larger output of the joint objective function, the fewer available U2U pairs, implying a reduced opportunity for R-UAVs' position optimization, could not provide sufficient contributions to system improvement, thus significantly offsetting the effect of PP reduction.

Therefore, from the two aspects above, a medium-to-high swarm velocity results in a higher  $P_p^{\text{tot}}$ , although its increment rate against velocity could be relatively lower under a greater  $d_{\min}$ . To maintain a low PP, we may select a relative low swarm velocity of around 10 m/s, as shown in Figure 3a.

Furthermore, Figure 3b shows that the total STR of H-UAVs  $R^{\text{tot}}$  reduces as the swarm velocity and/or  $d_{\min}$  become higher. Similar to our analysis for Figure 3a above, the reason for this phenomenon is also due to C3 and C7 in (11). Again, the increment of swarm velocity and  $d_{\min}$  will reduce the number of



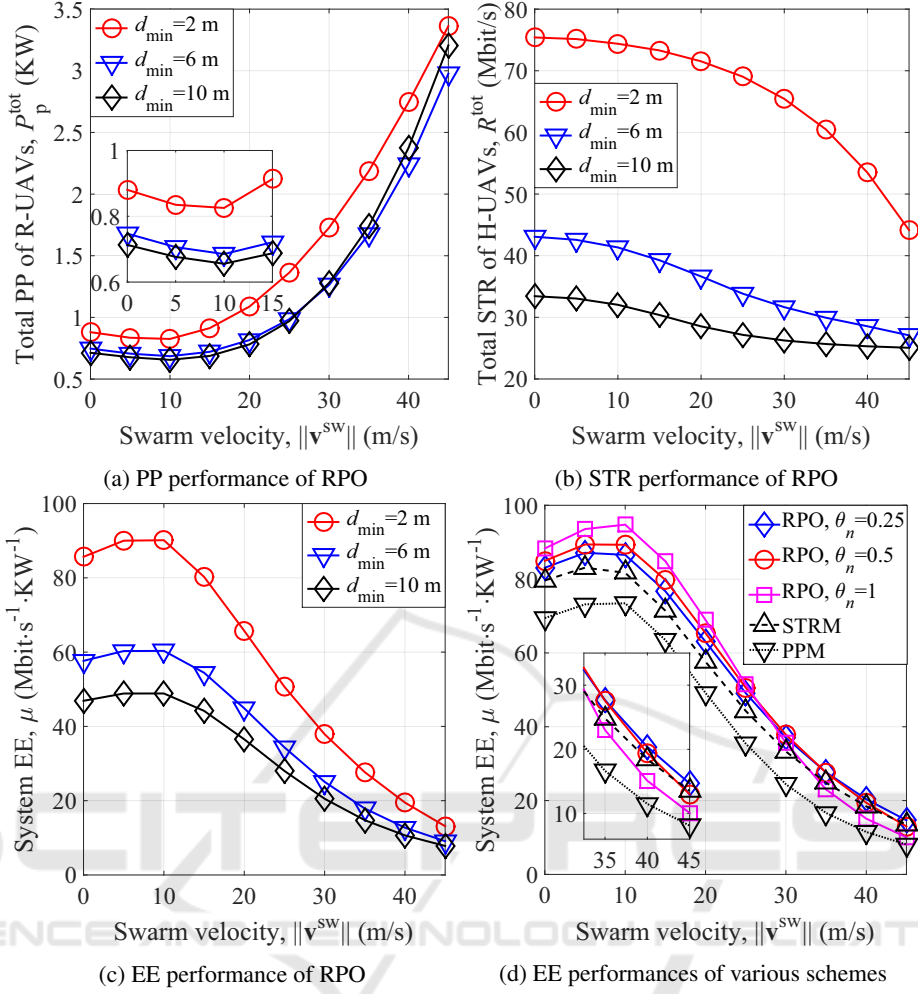


Figure 3: Performances of the IaS-U2U system supported by various algorithms.

R-UAVs qualified for U2U pairing, and thus affects the overall STR performance. Interestingly, Figure 3c illustrates that the EE  $\mu$  first increases and then reduces when the swarm velocity becomes larger, and that the shortest safety distance of  $d_{min} = 2$  m helps to achieve the highest  $R^{tot}$  and EE at the cost of a moderately increased PP compared with other larger values of  $d_{min}$ . Note that thanks to the rapid development of UAV technologies, the safety distance has been gradually reduced in recent years (Zhu et al., 2019), which may therefore provide a beneficial condition for the proposed RPO scheme.

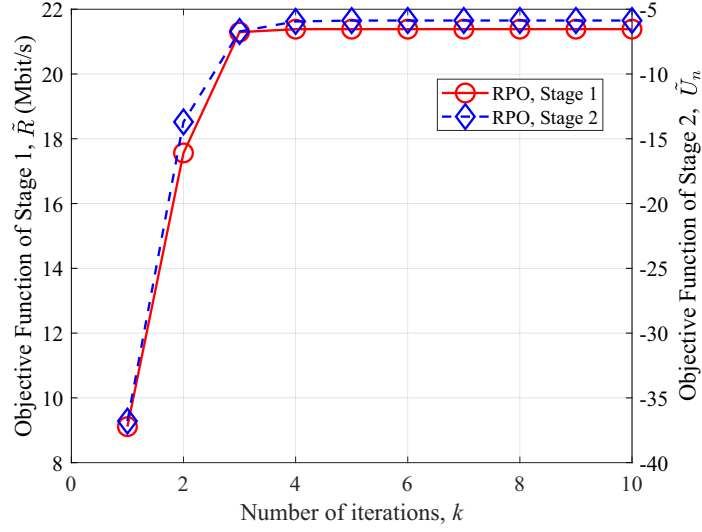
From Figure 3a, Figure 3b and Figure 3c, we can see that a performance tradeoff exists among  $P_p^{tot}$ ,  $R^{tot}$ ,  $\mu$  and  $\|v^{sw}\|$ , while RPO tends to balance these aspects of the IaS-U2U system. Last but not the least, it is worth pointing out that RPO can achieve a higher EE than the benchmarker schemes STRM and PPM, as proved by Figure 3d under  $d_{min} = 2$  m, where useful system design hints can be found. For example,

to achieve a higher EE, one may reduce (or increase) the priority factor  $\theta_n$  of RPO, when  $\|v^{sw}\|$  is lower (or higher) than the threshold of 32.5 m/s at the intersecting point of the various RPO curves associated with different  $\theta_n$ .

## 5.2 Complexity Analysis

Note that the computational complexity of the proposed RPO scheme in Algorithm 1 mainly depends on the interior-point method (IPM) (Nesterov and Nemirovskii, 1994), which yields a complexity of  $K_{iter} \cdot \log(1/\epsilon) \cdot O(n_{var}^{3.5})$  (Wang et al., 2020), where  $K_{iter}$ ,  $\epsilon$  and  $n_{var}$  denote the number of SCA iterations, the predefined accuracy of IPM and the number of variables, respectively.

For Stage 1 and Stage 2 of RPO, we have  $n_{var} = 2$  and  $n_{var} = 3$ , respectively. Naturally, if a higher RPO accuracy, denoted by  $\zeta$ , of the algorithm is targeted, a larger  $K_{iter}$  is required. Table 1 shows the average

Figure 4: The convergence of the RPO algorithm with  $K_{\max} = 10$ .

value of  $K_{\text{iter}}$  required for achieving a given RPO accuracy. In addition, recall that the objective functions of Stage 1 and Stage 2 in RPO are  $\tilde{R}$  in (28) and  $\tilde{U}_n$  in (26), respectively. Figure 4 shows that both of them become saturated after only a few iterations, indicating a good convergence of the RPO algorithm.

Table 1: The average number of SCA iterations required for achieving a given target RPO accuracy.

$\zeta$		$10^{-1}$	$10^{-2}$	$10^{-3}$
$K_{\text{iter}}$ (average)	Stage 1	3.6560	4.7625	8.6073
	Stage 2	2.5866	4.4713	7.7300

## 6 CONCLUSIONS

In this paper, an IaS-U2U communication mechanism is proposed for the OOC scenario, where a joint optimization problem is formulated by taking into account the STR and the PP. After decomposing the problem to the UAV pairing and the RPO processes, we devise a new two-stage algorithm to solve it. Simulations show that good EE gains can be achieved over selected benchmark schemes under various conditions. Our future research will extend this work to the scenario with multiple swarms.

## ACKNOWLEDGEMENTS

This work was supported by the Key-Area Research and Development Program of Guangdong Province under Grant 2019B010157002.

## REFERENCES

- 3GPP (2017). 3rd generation partnership project; technical specification group radio access network; study on enhanced LTE support for aerial vehicles; (release 15). TR 36.777 V15.0.0.
- 3GPP (2019). 3rd generation partnership project; technical specification group service and system aspects; enhancement for unmanned aerial vehicles; stage 1 (release 17). TR 22.829 V17.1.0.
- 3GPP (2020). 3rd generation partnership project; technical specification group core network and terminals; proximity-services (ProSe) user equipment (UE) to ProSe; stage 3 (release 16). TS 24.334 V16.0.0.
- Ahmed, S., Chowdhury, M. Z., and Jang, Y. M. (2020). Energy-efficient UAV-to-user scheduling to maximize throughput in wireless networks. *IEEE Access*, 8:21215–21225.
- Chen, Q. (2020). Joint position and resource optimization for multi-UAV-aided relaying systems. *IEEE Access*, 8:10403–10415.
- Chi, C. Y., Li, W. C., and Lin, C. H. (2017). *Convex Optimization for Signal Processing and Communications*. CRC Press.
- Du, B., Xue, R., Zhao, L., and Leung, V. C. (2020). Coalitional graph game for air-to-air and air-to-ground cognitive spectrum sharing. *IEEE Trans. Aerosp. Electron. Syst.*, 56(4):2959–2977.
- Gusfield, D. and Irving, R. W. (1989). *The Stable Marriage Problem: Structure and Algorithm*. MIT Press.
- Hong, L., Guo, H., Liu, J., and Zhang, Y. (2020). Toward swarm coordination: topology-aware inter-UAV routing optimization. *IEEE Trans. Veh. Technol.*, 69(9):10177–10187.
- Liu, A. and Lau, V. K. N. (2019). Optimization of multi-UAV-aided wireless networking over a ray-

- tracing channel model. *IEEE Trans. Wirel. Commun.*, 18(9):4518–4530.
- Nesterov, Y. and Nemirovskii, A. (1994). *Interior-point Polynomial Algorithms in Convex Programming*. SIAM, Philadelphia, PA, USA.
- Niwattanakul, S., Singthongchai, J., Naenudorn, E., and Wanapu, S. (2013). Using of Jaccard coefficient for keywords similarity. In *Proc. Int. Multi Conf. Eng. Comput. Sci.*, volume I, pages 380–384.
- Ranjha, A. and Kaddoum, G. (2020). Quasi-optimization of distance and blocklength in URLLC aided multi-hop UAV relay links. *IEEE Wirel. Commun. Lett.*, 9(3):306–310.
- Wang, H., Wang, J., Ding, G., Chen, J., and Yang, J. (2020). Completion time minimization for turning angle-constrained UAV-to-UAV communications. *IEEE Trans. Veh. Technol.*, 69(4):4569–4574.
- Ye, H.-T., Kang, X., Joung, J., and Liang, Y.-C. (2021). Optimization for wireless-powered IoT networks enabled by an energy-limited UAV under practical energy consumption model. *IEEE Internet Things J.*, 10(3):567–571.
- Zeng, Y., Xu, J., and Zhang, R. (2019). Energy minimization for wireless communication with rotary-wing UAV. *IEEE Trans. Wirel. Commun.*, 18(4):2329–2345.
- Zhang, S., Zhang, H., Di, B., and Song, L. (2019). Cellular UAV-to-X communications: design and optimization for multi-UAV networks. *IEEE Trans. Wirel. Commun.*, 18(2):1346–1359.
- Zhu, X., Liang, Y., and Yan, M. (2019). A flexible collision avoidance strategy for the formation of multiple unmanned aerial vehicles. *IEEE Access*, 7:140743–140754.